

# Thickness dependent structural and electronic properties of CuO adsorbed on SrTiO<sub>3</sub>(100): a hybrid density functional theory study

C. Franchini,<sup>1</sup> Xing-Qiu Chen,<sup>2</sup> and R. Podloucky<sup>3</sup>

<sup>1</sup> Faculty of Physics, Universität Wien and Center for Computational Materials Science, A-1090 Wien, Austria

<sup>2</sup> Shenyang National Laboratory for Materials Science, Institute of Metal Research, Chinese Academy of Sciences, 72 Wenhua Road, Shenyang 110016, China

<sup>3</sup> Institute for Physical Chemistry, Universität Wien, Sensengasse 8/7, A-1090 Wien, Austria.

(Dated: November 21, 2018)

We discuss the structural and electronic properties of tetragonal CuO grown on SrTiO<sub>3</sub>(100) by means of hybrid density functional theory. Our analysis explains the anomalously large Cu-O vertical distance observed in the experiments ( $\approx 2.7\text{\AA}$ ) in terms of a peculiar frustration between two competing local Cu-O environments characterized by different in-plane and out-of-plane bond lengths and Cu electronic populations. The proper inclusion of substrate effects is crucial to understand the tetragonal expansion and to reproduce correctly the measured valence band spectrum for a CuO thickness of 3-3.5 unit cells, in agreement with the experimentally estimated thickness.

PACS numbers: 68.35.bt, 73.61.Le, 71.15.-m

## I. INTRODUCTION

Very recently, Siemons *et al.*<sup>1</sup> synthesized CuO with a tetragonal (i.e. elongated rock salt structure) on a SrTiO<sub>3</sub>(100) substrate. In a subsequent theoretical study<sup>2</sup> we investigated bulk phases of tetragonal CuO by applying a hybrid density functional theory approach, which is able to deal with the electronic, ionic and magnetic properties of such a system. Studying a variety of magnetic orderings we obtained two energy minima as a function of tetragonal distortion. The antiferromagnetically ordered phase (denoted as TET2) with a tetragonal distortion of  $c/a=1.377$  appeared to be the most stable one with its lattice parameters being in very good agreement with the experimental results. Furthermore, for the TET2 phase we predicted a very high Néel temperature ( $T_N$ ) of 800 K, which would perfectly fit the trend of  $T_N$  for the 3d-transition metal monoxides<sup>1</sup>. Also, the calculated density of states of the TET2 phase agreed well with the experimental valence band spectrum with the exception of a few residual differences related to the structure of the main peak and the presence of an additional peak in the low energy spectrum which we have attributed to surface/substrate effects not taken into account in our previous analysis.

The aim of the present work is now, to corroborate our basic findings for the artificial TET2 phase by modelling experiment as realistically as possible. This is what we do by describing the adsorbate system in terms of an (CuO)<sub>[n]</sub>/SrTiO<sub>3</sub>(100) slab for varying thicknesses of CuO layers [with n denoting a CuO coverage of 2,3,3.5 and 4 unit cells (u.c.)].

Shortly after the publication of our bulk CuO study, a further theoretical study appeared, which was based on the self-interaction-corrected local-density functional method.<sup>3</sup> Again, for a variety of magnetic orderings two energy minima were found as a function of the tetragonal distortion, but the  $c/a$  values were much closer to

1 than in our work and, consequently, in worse agreement with the experimentally observed  $c/a$  ratio of 1.357. Therefore, the present study also serves the purpose to buttress the theoretical capability of our applied hybrid density functional theory approach and to understand the nature of the exceptionally large vertical elongation observed in SrTiO<sub>3</sub> supported CuO.

## II. COMPUTATIONAL ASPECTS

Because standard density functional theory applications fail in correctly describing the ground state of 3d-transition metal monoxides, a more sophisticated (and much more costly) approach has to be chosen. Therefore, for the present study we apply hybrid density functional theory<sup>4</sup> based on the Heyd-Scuseria-Ernzerhof (HSE) method<sup>5</sup> as implemented in the Vienna *ab initio* simulation package (VASP)<sup>6-8</sup>. All the corresponding technical parameters were the same as in our recent study<sup>2</sup> of tetragonal bulk CuO. In particular, 1/4 of short-ranged Hartree Fock exchange was admixed to the generalized-gradient-approximation exchange-correlation functional. The adsorbate systems (CuO)<sub>[n]</sub>/SrTiO<sub>3</sub>(100) (n=2,3,3.5 and 4 unit cells) were modelled by a repeated slab scheme containing up to 62 atoms per slab for the highest coverage. Figures 1 and 2 sketches the basic layer-wise atomic arrangements. All atomic positions of CuO layers were fully relaxed, whereas for the SrTiO<sub>3</sub> substrate the lowest 5 bottom layers, corresponding to a full SrTiO<sub>3</sub> unit cell, were kept fixed. The lateral lattice parameter  $a=3.90\text{\AA}$  for SrTiO<sub>3</sub> was taken from the recent VASP-based HSE study by R. Wahl and coworkers<sup>9</sup>. Indeed, the optimal HSE value of  $a$  is in very good agreement with the measured lattice constant  $a_{\text{Expt}}=3.900\text{\AA}$ <sup>10</sup>. In order to make the HSE computations feasible, ferromagnetic (FM) ordering was assumed although a specific antiferromagnetic ordering appeared to be energetically more stable in the ideal tetragonal bulk phase.<sup>2</sup> Nevertheless, also because

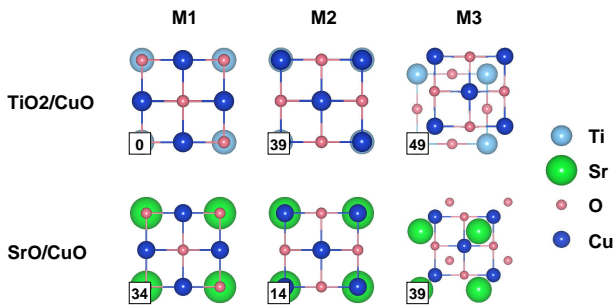


FIG. 1: (Color online) Top view of the interface models of the  $(\text{CuO})_{[n]}/\text{SrTiO}_3(100)$  adsorbate system as studied by the present HSE approach. The numbers in the squares (bottom left corner of each structure) denote the calculated energy difference (in  $\text{meV}/\text{\AA}^2$ ) relative to the  $\text{TiO}_2$  terminated M1 stacking, which is the most stable arrangement.

of the small magnetic Cu-moments of about  $0.7 \mu_B$  we expect only a small influence of the magnetic ordering on the structural relaxations and valence band spectrum<sup>11</sup>, which are the aim of study of our present work on the  $(\text{CuO})_{[n]}/\text{SrTiO}_3(100)$  substrate system. The  $\mathbf{k}$ -points integration for the structural optimization runs has been done by using a  $4 \times 4$  two dimensional Monkhorst-Pack grid, which was increased to  $6 \times 6$  for the final electronic relaxation.

### III. RESULTS AND DISCUSSION

#### A. Structural Properties

For finding the energetically most stable atomic arrangement several terminations of the  $\text{SrTiO}_3(100)$  substrate and stacking of the  $\text{CuO}$  adsorbate have been investigated. Fig. 1 sketches all the studied cases: the substrate is either  $\text{TiO}_2$  or  $\text{SrO}$  terminated.  $\text{CuO}$  layers may be accommodated in several ways: (i) Cu on top of oxygen atoms (M1), (ii) Cu on top of Ti or Sr atoms (M2) or (iii) Cu and O in hollow sites (M3). These (FM) calculations have been done by placing 2  $\text{CuO}$  unit cells (5  $\text{CuO}$  layers) on  $\text{SrTiO}_3$  (6 unit cells). Fig. 1 shows that the  $\text{TiO}_2$  terminated M1 structure is the most stable one. It should, however, be noted that rather close in energy (only  $14 \text{ meV}/\text{\AA}^2$  less stable) is the  $\text{SrO}$  terminated M2 stacking.

From now on, we only discuss the  $\text{TiO}_2$  terminated M1 structure. We study the evolution of the structural and electronic properties of the  $(\text{CuO})_{[n]}/\text{SrTiO}_3(100)$  adsorbate system for a  $\text{CuO}$  coverage of  $n=2,3,3.5$  and 4 unit cells. This choice is based on the experiments estimate, that a tetragonal  $\text{CuO}$ -layer consisting of 3 to 4 unit cells can be grown on  $\text{SrTiO}_3(100)$ <sup>1</sup>. The corresponding structural models are displayed in Fig 2.

The structural properties are summarized in Fig.3 and Table I. Fig. 3 illustrates that theoretical and experimental geometrical properties agree well when in the calcu-

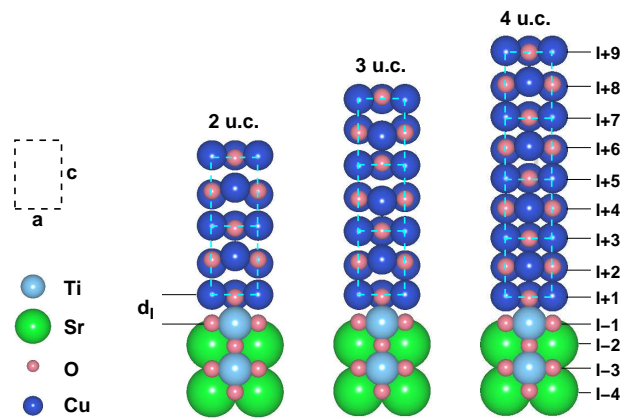


FIG. 2: (Color online) Side view of the  $(\text{CuO})_{[n]}/\text{SrTiO}_3(100)$  slabs for a coverage by  $n=2,3,4$  unit cells of  $\text{CuO}$  as used in the HSE calculation. (The  $n=3.5$  coverage, which was also studied, is not shown). Atomic arrangements according to the  $\text{TiO}_2$  terminated substrate and the M1 stacking of the  $\text{CuO}$  adsorbate (see Fig. 1). The layers are numbered with respect to the interface:  $I+j$  denotes  $\text{CuO}$  layers,  $I-j$  marks  $\text{SrTiO}_3$  layers. The side projected two dimensional unit cell with lattice parameters  $a$  and  $c$  is sketched by the dashed rectangle. Detailed structural data are listed in Table I.

lation the  $\text{CuO}$  coverage is 3.5 unit cells, which is also in the estimated range of the experimentally derived thickness (parameter D in Table I). The experimental value of  $c/a=1.357$  is close to the theoretical value of 1.345, which compares favorably to  $c/a=1.377$  as obtained from the HSE study for the ideal bulk TET2 phase.<sup>2</sup> In general, when increasing the number of unit cells  $c$  and  $c/a$  decrease as shown in Table I.

The analysis of the interlayer distances reveals that inside the  $\text{SrTiO}_3$  substrate the interface effects are healed out rather rapidly. Only the distance of the layer closest to the interface ( $d_{I-1/I-2}$ ) experiences a distinct shortening, as it is also the case for the  $\text{CuO}$  layer at the interface ( $d_{I+1/I-1}$ ). On the other hand, the  $\text{CuO}$  layer distances appear to be quite sensitive to the thickness of adsorbed  $\text{CuO}$ . For coverage of 2 and 3 unit cells the distances are significantly larger than the reference value of  $2.69 \text{ \AA}$  which was derived from the ideal TET2 bulk study. For coverage larger than 3 unit cells the distances between the inner  $\text{CuO}$  layers are significantly shortened, whereas the top 2 layers expand outwards. This change in bond length is reflected by the change of ionicity of Cu, as will be discussed in the following.

#### B. Electronic Properties

Figure 4 compares the HSE calculated density of states (DOS) with the experimental valence band spectrum. It is obvious that the total as well as the local  $\text{CuO}$ -projected DOS is rather sensitive to the thickness of the  $\text{CuO}$  block. Strikingly, the calculated DOS for the ideal TET2 bulk phase and for the system with  $n=3-3.5$  unit

TABLE I: Geometrical data for  $(\text{CuO})_{[n]}/\text{SrTiO}_3(100)$  for  $n=2, 3, 3.5$  and  $4$  ( $n$ : number of  $\text{CuO}$  unit cells). The data for  $c$  and  $c/a$  are based on averages of the vertical lattice parameter according to Ref. 1, and the lateral parameter  $a=3.90$  Å of  $\text{SrTiO}_3(100)$  is taken from another VASP-based HSE study<sup>9</sup>. The total thickness of adsorbed  $\text{CuO}$  is described by  $D$ . The interlayer distance between two subsequent layers as illustrated in Fig. 2 is denoted by  $d$ , and  $d_{I+1/I-1}$  indicates the interface separation between  $\text{SrTiO}_3$  and  $\text{CuO}$ . Layers are labelled according to Fig.2. The lattice parameters of the HSE calculation for the ideal TET2 phase<sup>2</sup> are  $a=3.908$  and  $c=5.381$  Å resulting in an ideal bulk-like layer distance of  $2.69$  Å. Experimental values are included when available. All length parameters are given in units of Å.

	2 u.c.	3 u.c.	3.5 u.c	4 u.c.	Expt. <sup>1</sup>
$c$	5.86	5.51	5.24	5.15	5.3
$c/a$	1.503	1.413	1.345	1.321	1.357
$D$	11.72	16.53	18.35	20.61	15-20
$d_{I+9/I+8}$				2.82	
$d_{I+8/I+7}$			2.87	2.70	
$d_{I+7/I+6}$		2.84	2.80	2.63	
$d_{I+6/I+5}$		2.78	2.61	2.56	
$d_{I+5/I+4}$	3.03	2.85	2.57	2.53	
$d_{I+4/I+3}$	2.93	2.72	2.49	2.46	
$d_{I+3/I+2}$	2.90	2.65	2.44	2.43	
$d_{I+2/I+1}$	2.93	2.73	2.58	2.49	
$d_{I+1/I-1}$	2.47	2.37	2.37	2.29	
$d_{I-1/I-2}$	1.88	1.88	1.86	1.82	
$d_{I-2/I-3}$	2.00	2.00	1.97	1.92	
$d_{I-3/I-4}$	1.95	1.94	1.94	1.90	
$d_{I-4/I-5}$	1.97	1.97	1.94	1.90	
$d_{I-5/I-6}$	1.98	1.94	1.95	1.92	
$d_{I-6/I-7}$	1.98	1.95	1.95	1.92	
$d_{I-7/I-8}$	1.95	1.95	1.96	1.94	
$d_{\text{bulk}}$	1.95	1.95	1.95	1.95	1.95

cells coverage agree well with experiment, quite in contrast to all cases. Though the superstructure with 2  $\text{CuO}$  u.c. already displays some film features which are not reproduced in the calculated bulk spectrum (such as the appearance of the peak A), the overall comparison with the measured curve is not satisfactory due to (i) a much too dominant presence of substrate-related states which weaken the intensity of the main  $\text{CuO}$  peaks around  $-4$  eV and (ii) the lack of a one-to-one correspondence between theoretical and experimental peaks.

As was discussed for the bulk phase TET2<sup>2</sup>, the agreement with experiment is rather good with the exception of one missing peak (indicated by the letter A in Fig. 4) and one extra peak (indicated by the cross) in the calculated spectrum. From the DOS for  $n=3-3.5$  one clearly

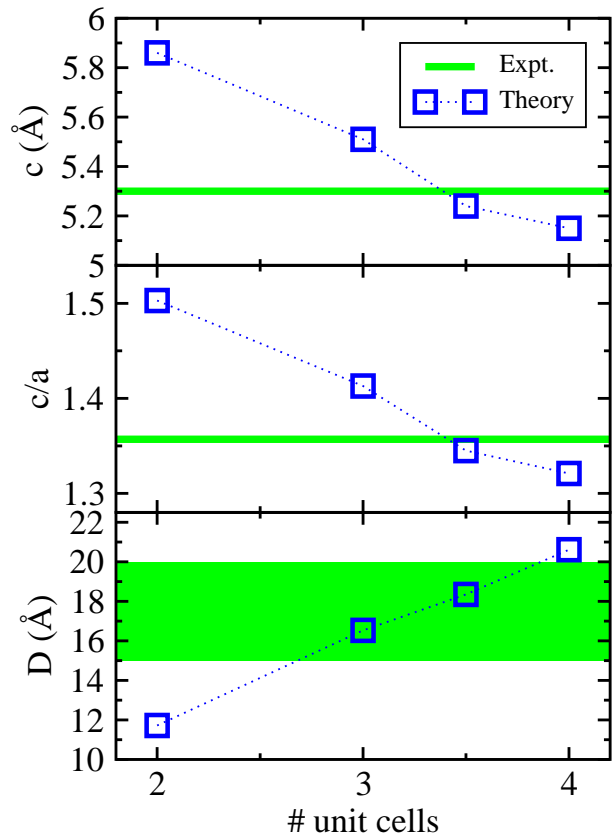


FIG. 3: (Color online) Thickness dependent variation of the structural parameters  $D$ ,  $c/a$  and  $c$  of the  $\text{CuO}$  adsorbate on  $\text{SrTiO}_3(100)$  as listed in Table I. Horizontal bars illustrate the experimental data of Ref.1.

deduces that the experimental structure is reproduced very well (especially for 3.5 u.c.) and the overall agreement is improved with respect to the ideal bulk phase. In particular, a new peak (A) is found due to the  $\text{CuO}$  interface layer (the local  $\text{CuO}$  DOS has a very distinctive peak at this energy position, which is also reflected in the total DOS) and the spurious peak found in the ideal bulk phase disappears. Finally, according to the DOS for  $n=3.5$  in Fig. 4 the highest experimental peak, can now be mainly attributed to the substrate, because there the local  $\text{CuO}$  DOS shows a weak depression, again in line with the observed valence band spectrum.

Figure 5 illustrates the layer dependent change of ionicity of the  $\text{Cu}$  atoms decomposed over the orbital quantum number  $l$ . A comparison with the corresponding bulk values for both the monoclinic and tenorite structures is also given. Leaving out the layer distance at the interface there is a uniform trend to be seen: with increasing distance from the interface the  $\text{Cu}$  charge is reduced by about  $0.15 e^-$  (i.e. the ionicity of the positive  $\text{Cu}$ -ions increases). This change in charge/valency (topmost panel) is mostly due to the change of p- and d-like charges (2nd and 3rd panel from the top). For the two  $\text{Cu}$  layers closest to the surface the total  $\text{Cu}$  charge

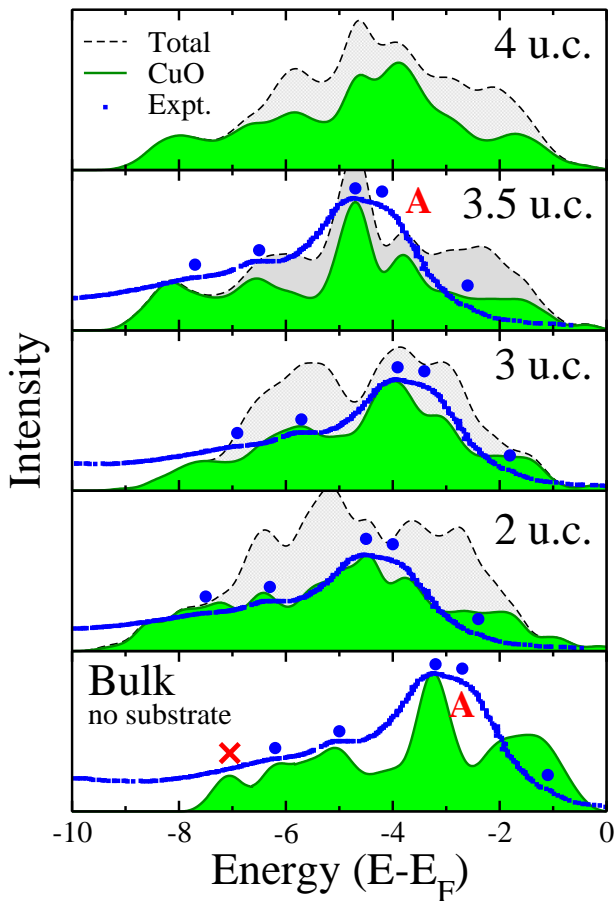


FIG. 4: (Color online) Results of the HSE calculations: total (light grey) and local CuO-projected (dark green) density of states for  $(\text{CuO})_{[n]}/\text{SrTiO}_3$  [ $n=2, 3, 3.5$  and  $4$  unit cells (u.c.)] and for the ideal bulk tetragonal TET2 phase.<sup>2</sup> The experimental curve is the valence-band spectrum of Ref.1. The circles and crosses indicate the position of the measured peaks. Energy zero is chosen to be the top of the valence band. Position of the maximum of the experimental spectrum is adjusted to the corresponding maximum of the HSE density of states. The calculated DOS is broadened by a Gaussian of half-width  $0.2$  eV.

is even less than for the tetragonal bulk phase. This increase in valency is directly accompanied by an increase in the interlayer distance, as clearly illustrated by Table I.

In general, an increase in bond length corresponds to an increase in ionicity: typical Cu-O bond lengths involving  $\text{Cu}^{2+}$  ions are of the order of  $2 \text{ \AA}$  whereas for  $\text{Cu}^{3+}$  the value might strongly increase up to  $2.75 \text{ \AA}$  (see Ref. 12). In our case, the increase in interlayer distance corresponds to the stretching of the Cu-O bond in the vertical direction (perpendicular to the Cu-O layers). According to Table I for the topmost layer of the  $n=3.5$  case the bond length is  $2.87 \text{ \AA}$ , being well in the bond length regime of  $\text{Cu}^{3+}$  ionicity. On the other hand, the in-plane bond lengths –due to the  $\text{SrTiO}_3$  substrate or the lattice parameter  $a=3.91 \text{ \AA}$  of the optimized bulk TET2 phase–

correspond rather well to an ionicity of  $\text{Cu}^{2+}$ . On the basis of our present surface and recent bulk TET2 study it seems that the Cu atoms appear in two competing concurrent ionic states, depending on the directions of the Cu-O bonds.

Our interpretation of the layer-dependent modulation of the Cu electronic population and Cu-O bond lengths suggesting a peculiar coexistence of  $\text{Cu}^{2+}$ -like and  $\text{Cu}^{3+}$ -like behavior is in line with the combined DFT and photoelectron spectroscopy study on copper oxide clusters presented by L.-S. Wang and coworkers<sup>13</sup>. By investigating the structural and electronic properties of  $\text{Cu}_2\text{O}_x$  ( $x=1-4$ ) these authors report a significant change both in the Cu-O bond length ( $0.05 \text{ \AA}$ ) and Cu charge ( $0.1e^-$ ) going from  $\text{Cu}_2\text{O}_2$  ( $\text{Cu}^{2+}$ ) to  $\text{Cu}_2\text{O}_3$  ( $\text{Cu}^{3+}$ ).

We can attribute the relatively small charge difference between bulk and surface Cu ions ( $0.15 e^-$ ), to the aforementioned competition between  $\text{Cu}^{2+}$ -like and  $\text{Cu}^{3+}$ -like environments. To support further this interpretation we have calculated the charge difference between  $2+$  and  $3+$  Mn ions in  $\text{MnO}$  and  $\text{Mn}_2\text{O}_3$  using the optimized data provided in Ref. 14. Indeed, the resulting value of  $0.38 e^-$ , by far smaller than the expected difference of 1 electron which would result from a simplified ionic picture, is twice larger than the corresponding Cu-difference in our frustrated  $\text{CuO}/\text{SrTiO}_3$  superstructure.

Finalizing the discussion of the electronic structure, the gap of the ideal TET2 phase of  $2.7 \text{ eV}$  is strongly reduced when CuO is grown on  $\text{SrTiO}_3$ : for a coverage of  $3.5$  unit cells the gap formed by CuO states is reduced to about  $0.6 \text{ eV}$ , which for the total system (now including substrate states) is even more reduced to about  $0.5 \text{ eV}$ . The average local magnetic moment for Cu is about  $0.75 \mu_B$ , which is enhanced in comparison to  $0.63 \mu_B$  of the bulk TET2 phase. It should be noted that the present calculation for the surface system  $(\text{CuO})_{[n]}/\text{SrTiO}_3(100)$  was done for ferromagnetic ordering (in order to make the HSE calculation feasible) whereas for the bulk TET2 calculation the most stable phase was found for some particular antiferromagnetic ordering<sup>2</sup>. However, in Ref. 2 studying several magnetic orderings it was found, that the local Cu moment is rather insensitive to the specific alignment of spins.

### C. Summary

Summarizing, our first principles study on the  $(\text{CuO})_{[n]}/\text{SrTiO}_3(100)$  adsorbate system based on a hybrid density functional theory approach describes and explains the recent experiments<sup>1</sup> rather well, which corroborates our findings and predictions for the ideal bulk (without  $\text{SrTiO}_3$  substrate) TET2 phase<sup>2</sup>. The analysis of our calculated results for structural and electronic properties indicates that the physical properties of the Cu-O bonds are rather peculiar. In particular, we find that the enormous structural anisotropy of the Cu-O sublattice –which determines the experimentally observed

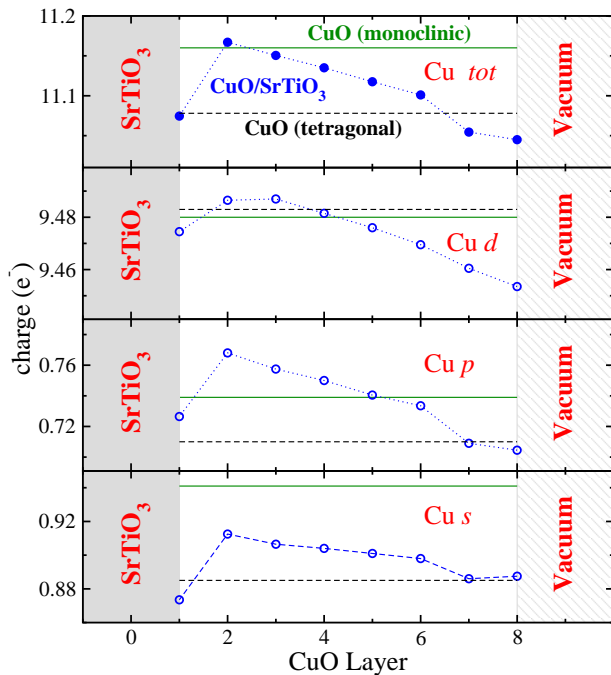


FIG. 5: (Color online) Layer by layer total and  $l$ -decomposed charge of Cu atoms (sphere radius of 1.16 Å) of  $(\text{CuO})_{[3.5]}/\text{SrTiO}_3(100)$  in comparison to the corresponding values for bulk monoclinic CuO (tenorite structure) and the ideal bulk tetragonal TET2 phase.<sup>2</sup> The placements of the  $\text{TiO}_3$  substrate and the vacuum regions are indicated.

tetragonal symmetry— can be understood in terms of a layer dependent evolution of the Cu ionicity which increases progressively towards the surface. Ultimately, the local structural and electronic Cu-O environment appears very frustrated as a result of the coexistence between two concurrent states attributable to an in-plane  $\text{Cu}^{2+}$ -like and out-of-plane  $\text{Cu}^{3+}$ -like arrangements.

#### IV. ACKNOWLEDGMENTS

Research in Vienna was sponsored by the FP7 European Community grant ATHENA. Support by the FWF, project nr. F4110-N13 is gratefully acknowledged. Research at the Shenyang National Laboratory for Materials Science was sponsored by the Materials Processing Modeling Division. X.-Q.C acknowledges the support from the Hundred Talents Project of Chinese Academy of Science. All calculations have been performed on the Vienna Scientific Cluster (VSC).

<sup>1</sup> W. Siemons, G. Koster, D.H.A. Blank, R.H. Hammond, T.H. Geballe, and M.R. Beasley, *Phys. Rev. B* **79**, 195122 (2009).  
<sup>2</sup> Xing-Qiu Chen, C.L. Fu, C. Franchini, and R. Podlucky, *Phys. Rev. B* **80**, 094527 (2009).  
<sup>3</sup> G. Peralta, D. Puggioni, A. Filippetti, and V. Fiorentini, *Phys. Rev. B* **80**, 140408(R) (2009).  
<sup>4</sup> A. D. Becke, *J. Chem. Phys.* **98**, 1372 (1993).  
<sup>5</sup> A. V. Krukau, *et. al.* *Chem. Phys.* **125**, 224106 (2006).  
<sup>6</sup> G. Kresse and J. Hafner, *Phys. Rev. B* **48**, 13115 (1993).  
<sup>7</sup> G. Kresse and J. Furthmüller, *Comput. Mater. Sci.* **6**, 15 (1996).  
<sup>8</sup> J. Paier, R. Hirschl, M. Marsman, and G. Jresse, *J. Chem. Phys.* **122**, 234102 (2005).

<sup>9</sup> R. Wahl, D. Vogtenhuber, and G. Kresse, *Phys. Rev. B* **78** 104116 (2008).  
<sup>10</sup> L. Cao, E. Sozontov, and J. Zegenhagen, *Phys. Status Solidi A* **181**, 387 (2000).  
<sup>11</sup> C. Franchini, J. Zabloudil, R. Podlucky, F. Allegretti, F. Li, S. Surnev, F.P. Netzer, *J. Chem. Phys.* **130**, 124707 (2009).  
<sup>12</sup> A.F. Well, *Structural Inorganic Chemistry*, 5th ed. (Oxford University Press, New York, 1987).  
<sup>13</sup> L.-S. Wang, H. Wu, S.R. Desai, and L. Lou, *Phys. Rev. B* **53** 8028 (1996).  
<sup>14</sup> C. Franchini, R. Podlucky, J. Paier, M. Marsman, and G. Kresse, *PRB* **75**, 195128 (2007).